Contents lists available at ScienceDirect

Heliyon

Single-cell RNA sequencing reveals neurovascular-osteochondral network crosstalk during temporomandibular joint osteoarthritis: Pilot study in a human condylar cartilage

Dahe Zhang [1], Yuxin Zhang [1], Simo Xia, Lu Chen, Weifeng Xu, Liang Huo, Dong Huang [***], Pei Shen [**], Chi Yang [*]

Department of Oral Surgery, Shanghai Ninth People's Hospital, Shanghai Jiao Tong University School of Medicine, College of Stomatology, Shanghai Jiao Tong University, National Center for Stomatology, National Clinical Research Center for Oral Diseases, Shanghai Key Laboratory of Stomatology, Shanghai Research Institute of Stomatology, Research Unit of Oral and Maxillofacial Regenerative Medicine, Chinese Academy of Medical Sciences, PR China

ABSTRACT

Purpose: Temporomandibular joint osteoarthritis (TMJ-OA) is one of the most complex temporomandibular disorders, causing pain and dysfunction. The main pathological feature of TMJ-OA is neurovascular invasion from the subchondral bone to the condylar cartilage. This study aimed to discover the cells and genes that play an important role in the neurovascular–osteochondral network crosstalk in human TMJ-OA.
Materials and methods: Condylar cartilages from patient with TMJ-OA were divided into OA group, and others from patients with benign condylar hyperplasia (CH) were used as control for further single-cell RNA-sequencing (scRNA-seq). Hematoxylin and eosin staining were performed. The cells and genes in the condylar cartilage were identified and analyzed by scRNA-seq.
Results: Histological analysis revealed blood vessel invasion and ossification in the TMJ-OA condylar cartilage. The scRNA-seq identified immune cells, endothelial cells, and chondrocytes in the TMJ-OA condylar cartilage. Macrophages, especially M1-like macrophages, contributed to the inflammation, angiogenesis, and innervation. CD31$^+$ endothelial cells contributed to the bone

mineralization. The TMJ-OA cartilage chondrocytes highly expressed genes related to inflammation, angiogenesis, innervation, and ossification. The hub genes contributing to these processes in the TMJ-OA chondrocytes included CTGF, FBN1, FN1, EGFR, and ITGA5.

Conclusion: Our study marks the first time scRNA-seq was used to identify the cells and genes in a human TMJ-OA condylar cartilage, and neurovascular–osteochondral network crosstalk during the human TMJ-OA process was demonstrated. Targeting the crosstalk of these processes may be a potential comprehensive and effective therapeutic strategy for human TMJ-OA.

1. Introduction

As the only movable joint in the maxillofacial region, the temporomandibular joint (TMJ) is important in complicated jaw movements, dental occlusion, and the neuromuscular system [1,2]. Different from other joints, the articular surface of the mandibular condyle in TMJ comprises fibrocartilage, which contains both type I and II collagen, denoting better loading capacity and healing potential [3,4]. Furthermore, the condylar cartilage is a secondary cartilage, indicating a different development and bone-formation process to other articular cartilages [2,5].

TMJ osteoarthritis (TMJ-OA) is a complex temporomandibular disorder that causes pain and dysfunction [6,7]. The characterizes of TMJ-OA include synovitis, cartilage degeneration, and subchondral bone changes [8–10]. However, the pathogenesis of TMJ-OA remains controversial, and the relevant etiology may be inflammation, mechanical stress, hormone, or genetic factors [11]. Previous studies demonstrated the regulatory relationship between cartilage and subchondral bone [12]. Considering the uniqueness of condylar cartilage in development, the change of condylar cartilage in TMJ-OA is widely investigated.

Several studies demonstrated that bottom–up innervation and angiogenesis can cross the tidemark from subchondral bone to cartilage, which is important in the cartilage erosion process of OA [9,12,13]. The mechanism of these changes has been widely studied. First, increased macrophage infiltration promotes angiogenesis by degrading cartilage matrix and producing proangiogenic factors [12,14]. Second, OA cartilage has weak resistance to vessel formation due to proteoglycan depletion and the proangiogenic factors produced by chondrocytes [15]. Third, the hypoxia environment of OA promotes the expression of hypoxia-inducible factor 1 (HIF-1) and its target genes, which can increase blood vessel formation [16]. Innervation is closely related to angiogenesis, and vascular cells and perivascular environment cells can generate various neural system development regulators, e.g., vascular endothelial growth factor (VEGF) [14,17]. Nerve growth involves molecules such as semaphorins, neuropilins, and plexins, which also contribute to vessel formation [18]. Given the close link of sensory nerve growth and angiogenesis, the abnormal innervation can explain the pain, which is one of the main symptoms in patients with TMJ-OA [14]. The altered extracellular matrix (ECM) around the invading vessels indicates that angiogenesis is related to ossification in OA cartilage [12,14,19]. These findings suggest that inflammation, angiogenesis, innervation, and ossification closely interact in OA development.

Although such neurovascular–osteochondral crosstalk is important during TMJ-OA occurrence and development, information in human degraded condylar cartilage is scarce. Several animal models have been established and studied to further investigate the process of TMJ-OA, including the induced, naturally occurring, and genetically modified models [20]. The induced models were most widely used in the investigation of TMJ-OA, such as intra-articular injection [21,22], surgical induction [23], and mechanical loading models [24]. However, no one animal model is sufficient for studying all features of TMJ-OA or fully represents the development of TMJOA in human beings [20]. Thus, in the present study, single-cell RNA sequencing (scRNA-seq) was performed to discover the relevant markers in the cell types of condylar cartilage from TMJ-OA patients. The hypothesis was that the neurovascular–osteochondral network crosstalk plays an important regulatory role in human TMJ-OA occurrence and development.

2. Materials and methods

2.1. Sample recruitment

The Ethics Committee of Shanghai Jiao Tong University School of Medicine approved the use of human tissues (SH9H-2019-T189-2). One condylar cartilage from a patient with TMJ-OA was divided into OA group, and another condylar cartilage from a patient with benign condylar hyperplasia (CH) was used as control for further scRNA-seq. Signed informed consent was obtained from the patients.

2.2. Histopathological analysis

The patients' TMJ condyles were fixed in 4 % (w/v) paraformaldehyde for 48 h. The samples were decalcified in 10 % (w/v) Tris-EDTA buffer (Beyotime) at 37 °C until the tissues had softened. Then, the samples were dehydrated, paraffin-embedded, sliced into 5-μm thick sections, and positioned on glass slides. The slices were stained with hematoxylin and eosin (H&E, Sigma-Aldrich) for general morphology evaluation.

2.3. scRNA-seq data preprocessing

The patients' condylar cartilages were collected for scRNA-seq. Our previous study has reported the ectoderm chondrogenic cells

(ECCs), induced from H1 human pluripotent stem cells [25], and the scRNA-seq data was downloaded from the National Genomics Data Center Genome Sequence Archive (accession number HRA003116). The Cell Ranger software pipeline (version 5.0.0 10 × Genomics) was used to demultiplex cellular barcodes, map reads to the genome and transcriptome using the STAR aligner, and downsample reads to generate normalized aggregate data across samples, producing a gene count versus cell matrix. R 4.1.0 (https://www.R-project.org/) [26] was used for data preprocessing and further analysis. Data were preprocessed with the R package *Seurat* (version 3.1.1) [27]. The unique molecular identifier (UMI) count matrix was processed. The first quartile (Q1), third quartile (Q3) and interquartile range (IQR) of the UMI and gene numbers in each sample were calculated. Cells with UMI or gene numbers less than Q1-1.5 × IQR or more than Q3+1.5 × IQR were filtered out. Cells with >10 % of counts belonging to mitochondrial genes were removed. Potential doublets were removed using *DoubletFinder* package (version 2.0.2) [28]. The data were integrated using the *harmony* package [29], and normalized and scaled with the *NormalizeData* and *ScaleData* function. The 2000 most variable genes were selected using the FindVariableGenes function and were used for principal component analysis (PCA) and t-distributed stochastic neighbor embedding (tSNE) dimensional reduction by the RunHarmony and RunTSNE functions, respectively, to visualize the cells. The cells were clustered using the FindNeighbours and FindClusters functions. The genes expressed in at least 25 % of cells within the clusters and with log2(fold change) > 0.25 were identified as differentially expressed genes (DEGs) with the FindAllMarkers function. The upregulated DEGs in each cluster were used for further analysis.

2.4. Gene enrichment analyses

Gene Oncology (GO) term and Kyoto Encyclopedia of Genes and Genomes (KEGG) enrichment analyses of the DEGs were performed by the org.Hs.eg.db, clusterProfiler, and tidyverse packages. DEG gene set enrichment analysis (GSEA) was performed using the clusterProfiler package gseGO function [30]. For GSEA, the normalized enrichment score (NES) and adjusted P-value (false discovery rate) were reported. Based on the Molecular Signatures Database, gene set variation analysis (GSVA) was performed with the GSVA package [31].

2.5. Cell cycle analysis

Based on S- or G2/M-phase marker expression in each cell, the cell cycle status of each cell was identified using Seurat CellCycleScoring. The cell cycle score of each cell was visualized in a tSNE plot.

2.6. Pseudotime trajectory construction

The pseudotime trajectory was constructed using the Monocle2 package [32]. The Seurat object was established and quality-controlled as mentioned previously. Then, the expression matrix was extracted from the object and converted into a monocle object using the newCellDataSet function. The DEGs between the cells collected at the beginning and end of the process were determined using the differentialGeneTest function. Subsequently, the dimension of the object was reduced using the DDRTree method with the reduceDimension function. Next, the cells were ordered according to the DEGs and cell trajectory with the orderCells function. The DEGs among cells in different trajectory lineages were detected using the BEAM function. The DEGs were visualized by the plot_genes_branched_heatmap function and DEGs in similar lineage-dependent expression patterns were clustered together.

2.7. CytoTRACE

The *CytoTRACE* package [33] can be used to predict the relative cell differentiation potential. The differentiation potential scores of each cell were determined using the CytoTRACE function. The cells were re-clustered by the plotCytoTRACE function, where a higher score indicated a higher differentiation potential.

2.8. Metabolism pathways analysis

The cell activity score of each metabolic pathway was determined by the scMetabolism package sc.metabolism.Seurat function. The results are depicted in a dot plot and tSNE plots.

2.9. Protein-protein interaction (PPI) network construction

The PPI network was constructed using the Search Tool for the Retrieval of Interacting Genes/Proteins (STRING, https://string-db.org/) database. The DEGs of interest were converted into the database and the PPI network was visualized using Cytoscape (version 3.8.0) [34]. The degree of each node was determined by the cytoHubba plugin. The top 10 genes were identified as hub genes, where their expression levels are depicted in violin plots.
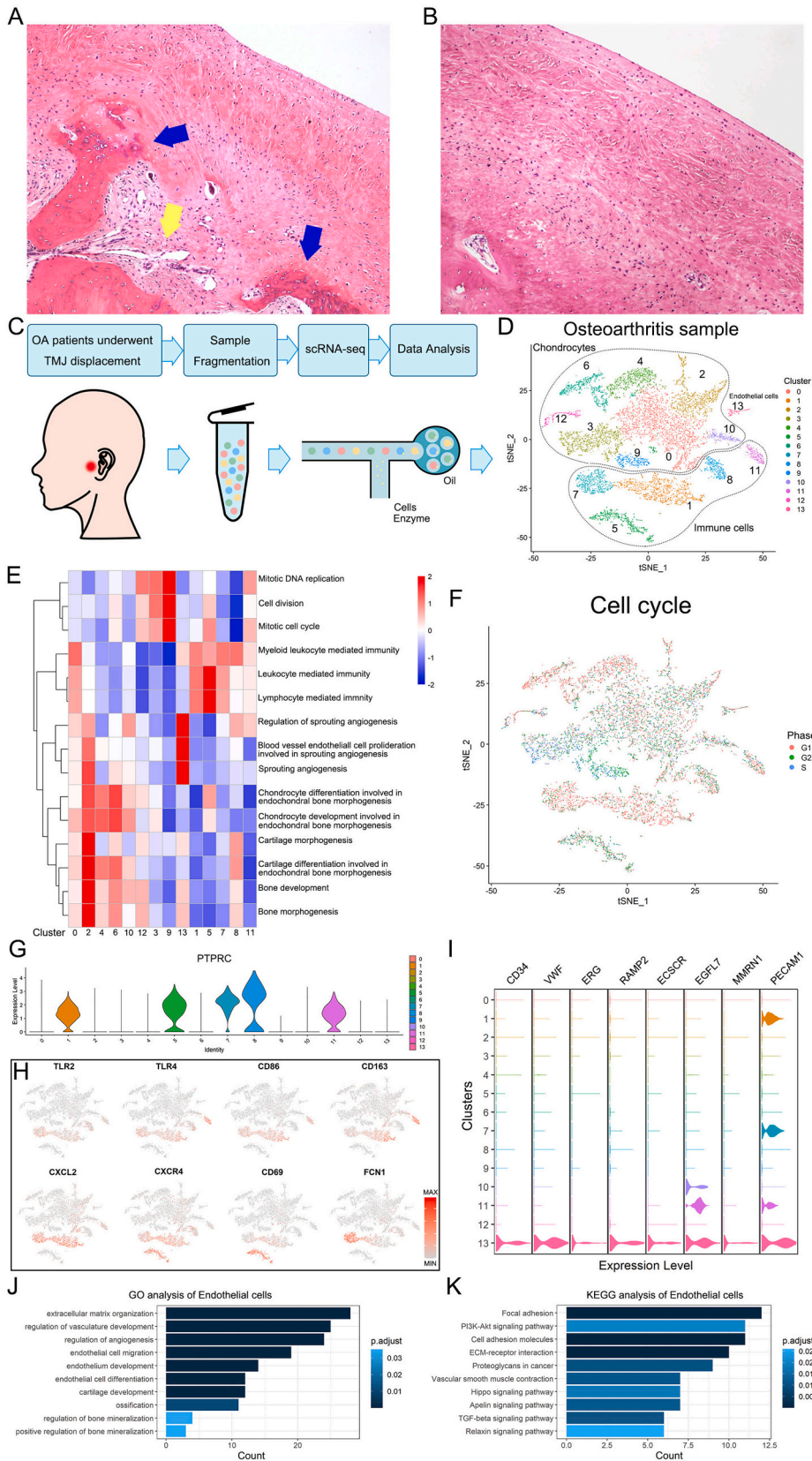
(caption on next page)

Fig. 1. Histopathological analysis of OA and CH cartilage, and scRNA-seq analysis of OA cartilage. (A, B) H&E staining of OA (A) and CH (B) cartilage. (C) scRNA-seq workflow. (D) Chondrocytes, immune cells, and endothelial cells identified in OA cartilage. (E) GSVA of the clusters in the GO terms related to mitosis, immunity, angiogenesis, and chondrocytes. (F) Cell cycle phases of the OA cells. (G) PTPRC (CD45) expression levels in the clusters. (H) Highly expressed immunity-related genes in OA cells. (I) Expression levels of endothelial cell markers in different cell clusters. (J) GO analysis of endothelial cells (Cluster 13). (K) KEGG analysis of endothelial cells (Cluster 13).

3. Results

3.1. The pathological changes in TMJ-OA condylar cartilage

The pathological changes in TMJ-OA condylar cartilage were validated with histopathological analysis. The H&E staining demonstrated the rough surface, blood vessel invasion, and ossification regions in the TMJ-OA condylar cartilage. The OA cartilage layers were indistinct and chondrocyte distribution was disorderly (Fig. 1A). The CH cartilage exhibited a smooth surface and the chondrocytes were homogenously distributed without blood vessels and ossification regions (Fig. 1B). The histopathological study demonstrated the important pathological changes, especially invasive angiogenesis, and abnormal ossification in TMJ-OA condylar cartilage.

3.2. Cell types in the TMJ-OA condylar cartilage

To identify the cellular components involved in the pathological changes of TMJ-OA condylar cartilage, scRNA-seq was performed on the condylar cartilage from a patient undergoing TMJ replacement (Fig. 1C). An initial 11,994 cells were sequenced from the sample, and 9808 cells remained after filtration, which were divided into 14 clusters. Three cell types were identified: chondrocytes, immune cells, and endothelial cells (Fig. 1D). GSVA determined the GO enrichment results corresponding to each cell type (Fig. 1E). The largest numbers of cells were chondrocytes, for which the cartilage- and bone mineralization-related GO terms were enriched. Among them, Cluster 3 and 9 exhibited high mitosis activity and were mainly in the mitotic G2/M or S phase (Fig. 1F). Therefore, these cells were considered cartilage progenitor cells (CPCs). Except for the chondrocytes, five clusters that highly expressed PTPRC (also known as CD45) and other immune-associated genes were identified as immune cells (Fig. 1G and H). Cluster 13, which highly expressed PECAM1 (also known as CD31), CD34, and VWF, was identified as endothelial cells (Fig. 1I). Upregulated DEGs in the endothelial cells were enriched in the GO terms related to angiogenesis, cartilage development, and ossification (Fig. 1J) and were enriched in the focal adhesion and PI3K–Akt signaling pathways (Fig. 1K).

### 3.3. Immune cells in TMJ-OA condylar cartilage

A total of 3000 immune cells were isolated for analysis and eight clusters were identified (Fig. 2A). Clusters 0, 1, 4, and 5 were identified as macrophages expressing marker genes (CD68, CD86, and CXCL8). The other clusters were Cluster 2, T cells expressing CD3D and CD3E; Cluster 3, neutrophils expressing NDA, S100A8, and CXCR2; Cluster 6, natural killer cells expressing NKG7, GNLY, and GZMA; and Cluster 7, B cells expressing CD19, CD79A, and MZB1 (Fig. 2B). The results demonstrated that macrophages mainly expressed the markers associated with angiogenesis and innervation (Fig. 2C and D).

The macrophages accounted for 64.9 % (1946 cells) of the total immune cells, and almost maintained the four initial clusters after re-clustered (Fig. 2E). APOC1+, FCN1+, C1QB+, and LYVE + macrophages were identified based on the highly expressed genes (Figs. S1A and S1B) and GO enrichment results (Fig. 2F) in each cluster, and considered Cluster 0, 1, and 4 M1-like macrophages, while Cluster 5 was M2-like macrophages.

Pseudotime trajectory construction revealed that the LYVE + macrophages were distributed in the trajectory root while the C1QB + macrophages were in the trajectory Pre-branch. The APOC1+ and FCN1+ macrophages entered two different cell fates (Fig. 2G). This trajectory indicated the change from M2-like macrophages to M1-like macrophages. The Pre-branch highly expressed M2 macrophage markers (MS4A4A, DAB2) and other genes that indicated inflammatory activity (C1QB, A2M). Cell Fate 1 demonstrated the strongest immune activity, as the upregulated genes in the Cell Fate 1 lineage were mainly enriched in the inflammation-related GO terms: positive regulation of cytokine production, IL-1β production, and IL-12 production. Genes up-regulated in Cell Fate 2 was mainly enriched in the lipid metabolism and immunity-related GO terms (Figs. S1C–E). The results indicated that macrophages are important in inflammation, angiogenesis, and innervation in the TMJ-OA process.

3.4. Chondrocytes in the TMJ-OA condylar cartilage

The 6667 chondrocytes in the TMJ-OA cartilage, which were the main cellular components of OA cartilage, were re-clustered into five clusters (Fig. 3A). Based on the highly expressed genes in the clusters (Fig. 3B), Cluster 3, which expressed CDC20, UBE2C, and BIRC5, was identified as CPCs (Fig. 3C). GO analysis and GSEA demonstrated that Cluster 3 had high RNA catabolic and mitosis activity (Fig. 3D and E). Cluster 0 expressed genes involved in immunity, angiogenesis, neurogenesis, and ossification (Fig. 3F). Cluster 1 exhibited high mitochondrial activity (Fig. 3G). The genes highly expressed in Cluster 2 were related to ECM organization, angiogenesis, ossification, and cellular response to hypoxia (Fig. 3H). Cluster 4 demonstrated high innervation, angiogenesis, and ossification activity (Fig. 3I). CytoTRACE confirmed the high development potential of Cluster 3 (Fig. 4A). The pseudotime trajectory
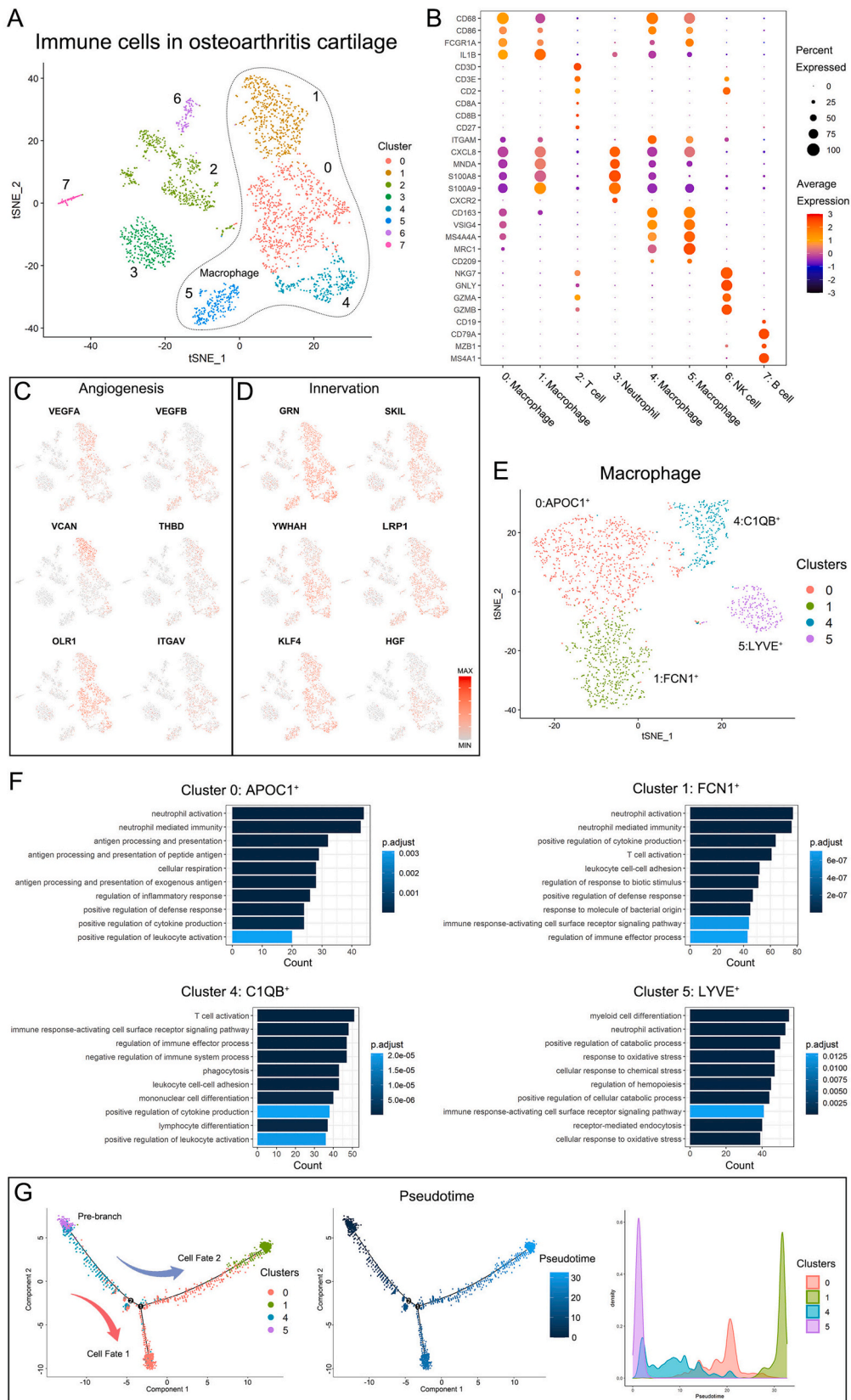
(caption on next page)

Fig. 2. Analysis of immune cells in OA cartilage. (A) Re-clustered 3000 immune cells isolated from OA cells. (B) Expression levels of immune cell markers and identification of the cell types in each cluster. tSNE was performed for highly expressed genes related to angiogenesis (C) and innervation (D). (E) Re-clustered 1946 macrophages isolated from immune cells and the most highly expressed genes in the four clusters. (F) GO analysis of macrophages in the four clusters. (G) Reconstructed pseudotime trajectory of the macrophages.

demonstrated that Clusters 3 and 1 were distributed in the trajectory root, Cluster 0 was mainly distributed in Cell Fate 1, Cluster 2 was distributed along Cell Fate 2, and Cluster 4 was at the end of Cell Fate 2 (Fig. 4B). Pre-branch cells expressed STMN1, RPLP1, and RPS18 and exhibited high mitochondrial activity. The genes highly expressed in Cell Fate 1 were mainly enriched in immune-related GO terms. Cell Fate 2 exhibited high catabolic activity (Fig. 4C–E).

3.5. Benign CH cartilage chondrocytes

The benign CH cartilage was obtained from a patient to use as a sample resembling normal cartilage as the control. The 11,058 cells were divided into five clusters (Fig. S2A). Except for Cluster 3, which demonstrated immune cell characteristics, the other cell clusters exhibited chondrocyte characteristics (Fig. S2B). The clusters were: Cluster 0, chondrocytes expressing PTN and OGN; Cluster 1, chondrocytes expressing RGS5 and COL4A1; Cluster 2, chondrocytes expressing IFI27 and PECAM1; Cluster 3 (372 cells), immune cells expressing CCL4 and CXCL8; Cluster 4, CPCs expressing TOP2A and STMN1 (Fig. S2C). Genes highly expressed in Cluster 0, were enriched in the GO terms related to ECM or bone development (Fig. S2D). Cluster 4 demonstrated high DNA replication and mitosis activity similar to the OA chondrocyte CPCs (Fig. S2E). There were almost no endothelial cells in the CH cartilage.

3.6. Comparison among ECC, CH and OA chondrocytes

The ECC (5123 cells), CH (10686 cells), and OA (6667 cells) chondrocytes were combined for further analysis. After merging, the chondrocytes maintained a high consistency with the previous clusters (Fig. S3A). The chondrocytes were re-clustered into seven clusters: CH0 and CH2 were re-clustered as CH-1, expressing MGP and SFRP2; CH1 was re-clustered as CH-2, expressing RGS5 and IGFBP7; OA0 was re-clustered as OA-1, expressing SPP1 and IGFBP1; OA2 and OA4 were re-clustered as OA-2, expressing PAPPA2 and NOTUM; OA1 was re-clustered as OA-3, expressing PAGE4 and PEG10; OA3, CH4 and a part of the ECCs were identified as CPCs, expressing STMN1, and UBE2C; other ECCs were clustered to ECC, expressing IGFBP2, NUPR1, and IGFBP5 (Fig. 5A and B, S3B). Highly expressed genes in OA-1 were enriched in the innervation-, inflammation-, and ossification-related GO terms (Fig. 5C). Highly expressed genes in OA-2 were involved in innervation, angiogenesis, inflammation, and ossification (Fig. 5D). OA-3 demonstrated high mitochondrial activity and indicated a hypoxia condition (Fig. S3C). The CH sample was used as the control, where CH-1 exhibited high cartilage and bone development activity (Fig. S3D). The ECC and CPCs demonstrated high glycolysis/gluconeogenesis and glycerolipid metabolism activity. The CHs exhibited high thiamine and primary bile acid biosynthesis activity. OA-1 demonstrated high glycosphingolipid biosynthesis, histidine metabolism, and linoleic acid metabolism activities. OA-2 showed high glyco-sphingolipid biosynthesis, glycan biosynthesis, and histidine metabolism activities. OA-3 had high oxidative phosphorylation, tryptophan metabolism, and tyrosine metabolism activities (Fig. S3E). The ECC and CPCs were considered to have differential potential and were in the pseudotime trajectory root. The OAs and CHs were in the Cell Fate 1 and 2 linages, respectively (Fig. 5E). The Cell Fate 1 upregulated DEGs were similar to that in the OAs and were enriched in the reactive oxygen species (ROS)-related, oxidative phosphorylation, and HIF-1 signaling KEGG pathways. The Pre-branch and Cell Fate 2 upregulated DEGs demonstrated similar enrichment in KEGG analysis, including the focal adhesion and PI3K–Akt signaling pathways (Fig. 5F and G). Compared with ECCs and CH cartilage, the TMJ-OA cartilage chondrocytes exhibited close inflammation, immunity, angiogenesis, and ossification crosstalk.

3.7. PPI network analysis of TMJ-OA condylar cartilage DEGs

PPI networks were constructed with the STRING database to analyze the OA cartilage hub genes and their mutual regulation. The highly expressed genes in the OA chondrocytes related to inflammation (Fig. 6A), innervation (Fig. 6B), angiogenesis (Fig. 6C), and ossification (Fig. 6D) were analyzed separately. Among these selected upregulated DEGs, the genes with log2(fold change) > 2 were analyzed together (Fig. 6E). Ten hub genes were selected by cytoHubba in Cytoscape: CTGF, FBN1, FN1, EGFR, ITGA5, HSPG2, SERPINE1, COL4A2, TIMP2, and IGFBP3 (Fig. 6F). The expression levels of these genes in the clusters are shown (Fig. 6G). These results indicated the strong neurovascular–osteochondral network crosstalk in the TMJ-OA condylar cartilage.

4. Discussion

The vascular invasion, innervation, and ossification in OA cartilage received extensive attention in recent studies [9,11–14]. Consistent with this, the present study detected blood vessel invasion and ossification regions in TMJ-OA cartilage via the H&E staining. Previously, strong interactions were detected among inflammation, innervation, and angiogenesis in rat TMJ-OA cartilage [17]. However, the DEG expression and interaction in different cell types in TMJ-OA cartilage are unknown, especially in human TMJ-OA cartilage. Accordingly, the present study aimed to identify the cell types and their contributions to neuro-vascular–osteochondral network crosstalk in human TMJ-OA condylar cartilage.

Although several studies have reported a variety of animal models to further investigate the process of TMJ-OA [20,21], there was a
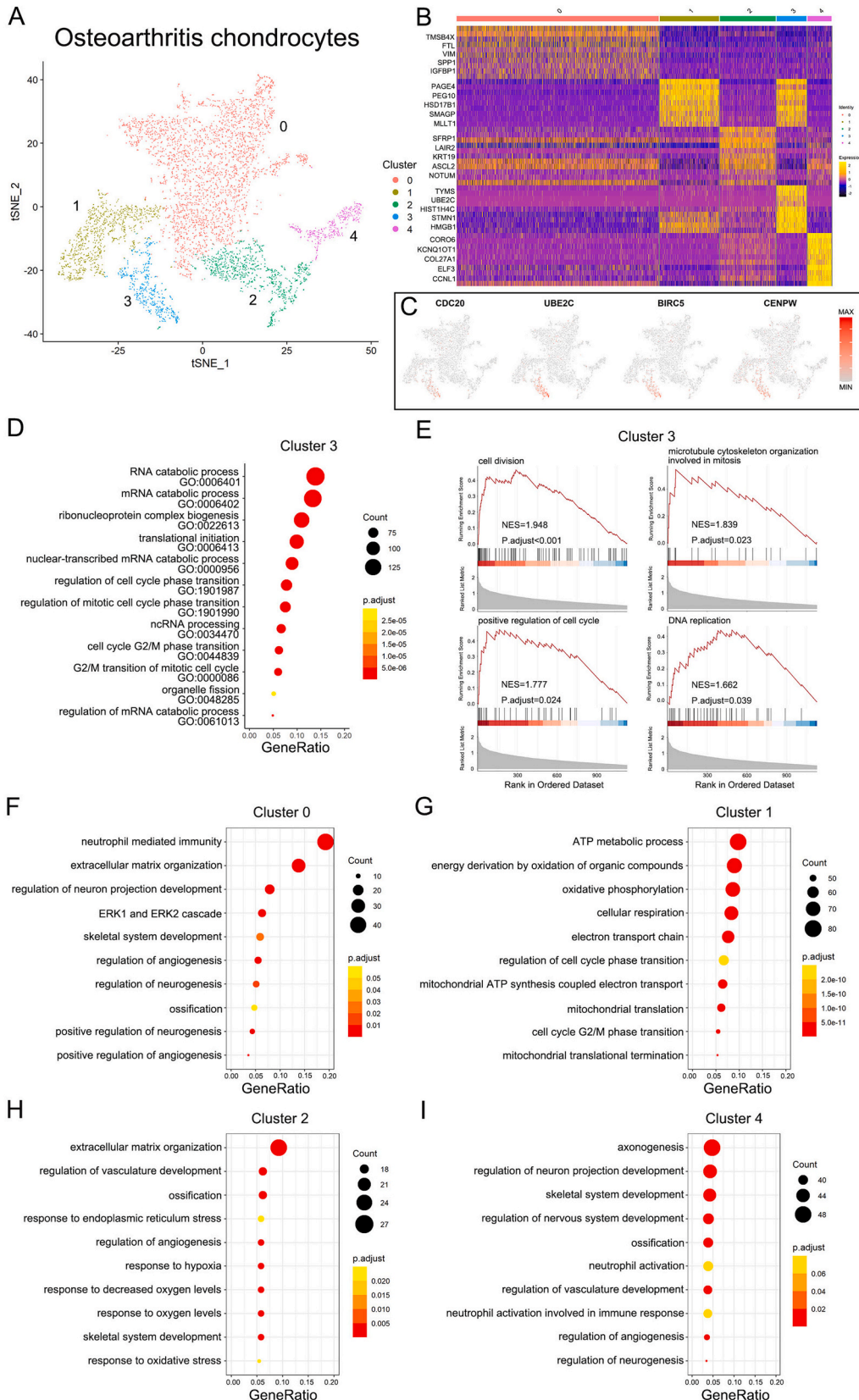
(caption on next page)

Fig. 3. Analysis of chondrocytes in OA cartilage. (A) Re-clustered 6667 chondrocytes. (B) DEGs in the five clusters. (C) High CDC20, UBE2C, BIRC5, and CENPW expression levels in Cluster 3. (D) GO analysis of Cluster 3. (E) GSEA of Cluster 3. (F–I) GO analysis of Cluster 0 (F), Cluster 1 (G), Cluster 2 (H), and Cluster 4 (I).

lack of studies that directly investigated the development of TMJ-OA in human beings. Thus, in our study, scRNA-seq deeply exhibited the changes of cells and genes in human TMJ-OA condylar cartilage. The results confirmed the existence of immune cells and endothelial cells in the human TMJ-OA condylar cartilage. Compared with this result, only 372 immune cells and no endothelial cells in the CH cartilage were identified. Macrophages were the main immune cell population in the TMJ-OA cartilage, specifically M1-like macrophages. The macrophage contribution to inflammation was analyzed in detail. Consistent with the traditional concept that macrophage infiltration contributes to angiogenesis [14], the macrophages highly expressed the important proangiogenic factors: VEGFA, VEGFB, and VCAN. However, the OA chondrocytes highly expressed the VEGF receptor FTL1, but not the VEGFs. An important study by Wan et al. [17], reported high VEGF expression in rat TMJ-OA condylar cartilage using microarray-based transcriptome analysis. Therefore, the results indicated that the high VEGF expression was mainly attributed to the macrophages, indicating their important role in angiogenesis in late-stage TMJ-OA condylar cartilage. In addition to the effect of VEGFs on innervation [14], the macrophages also expressed some essential innervation-related genes. Accordingly, the present study indicated that macrophages are important in inflammation, angiogenesis, and innervation during TMJ-OA development.

Cartilage ossification is another important pathological process in TMJ-OA [6,35]. The main population of OA chondrocytes exhibited high ossification activity. Vascularization promoted cartilage ossification [6]. Type H blood vessels, which highly expressed CD31 and endomucin, are of great concern due to its ability to modulate osteogenesis [36]. In our study, a cluster of cells expressing CD31 was identified, which contributed to the bone mineralization and cartilage development according to GO analysis. Except for the macrophages and endothelial cells, the OA condylar chondrocytes also expressed genes contributing to angiogenesis, innervation, and inflammation. This finding was of great concern, as it might be the core reason for the cartilage degeneration and ossification. The hub genes related to these processes were selected via the PPI network. CTGF is significantly highly expressed in OA joints and causes chondrocyte degeneration. The CTGF antibody pamrevlumab may be a potential drug for OA [37]. Fibronectin (FN1), which mediates various cellular interactions in the ECM, was upregulated in OA cartilage [38]. Wei Y et al. [39] reported the feasibility of targeting the EGFR pathway for OA therapy. Perlecan (HSPG2) is essential in OA osteophyte development [40]. These reports enhanced our findings. The other hub genes were less reported in OA cartilage, and IGFBP3 and COL4A2 play roles in ossification [41,42]. Further studies are needed to determine the role of the hub genes in OA. Nevertheless, the present study provides evidence that inflammation, angiogenesis, innervation, and ossification are accompanied by TMJ-OA condylar cartilage degradation and identified hub genes that may be important in these processes.

As mentioned previously, ECM protein downregulation led to weak resistance to vessel formation in OA cartilage [14]. Furthermore, hypoxia contributed to angiogenesis, ROS production, and mitochondrial activation [43,44]. Consistent with these previous findings, the present study demonstrated downregulated focal adhesion, ECM receptor interaction, and proteoglycan-related pathways in TMJ-OA condylar chondrocytes. Additionally, a cluster of TMJ-OA condylar chondrocytes exhibited high mitochondrial, oxidative phosphorylation, and ROS production activity and indicated a hypoxia environment. These findings demonstrated the correlation among angiogenesis, hypoxia, ROS production, and high mitochondrial activity. Nevertheless, further studies are needed to confirm these findings.

Inflammation and the infiltration of blood vessels and sensory nerve endings from subchondral bone to cartilage mainly cause the pain and structural damage in OA [6,14,45]. Many studies reported treatments targeting these pathological processes and related hub genes [12,14]. For example, the VEGF antibody bevacizumab inhibited vascular invasion and cartilage destruction in OA, and other antiangiogenic factors also exerted similar effects on cartilage protection [9,12,46]. Nonsteroidal anti-inflammatory drugs (NSAIDs) were first recommended for managing OA, where NSAID inhibition of COX-2 reduces OA inflammation, angiogenesis, osteogenesis, and pain [12]. Therefore, targeting the inflammation, angiogenesis, and innervation processes can inhibit cartilage ossification and destruction and reduce pain. Therapies targeting the crosstalk of these processes may be a potential treatment strategy for TMJ-OA.

Moreover, the chondrocytes in OA showed a different metabolism activity. Chondrocytes in OA that highly expressed SPP1 and IGFBP1 showed high glycosphingolipid biosynthesis and histidine metabolism activities, as did those with high expression of PAPPA2 and NOTUM. The important role of glycosphingolipid biosynthesis has been reported in few studies [47], but still needs further investigations. In knee OA, the change of histidine has been reported in serum or synovial fluid, but its mechanism remains further studies [48,49]. Other chondrocytes that highly expressed PAGE4 and PEG10 showed high tryptophan metabolism, and tyrosine metabolism activities. The change and disturbance of tryptophan metabolites may be related to the development of OA [50,51]. In addition, it has been reported that tyrosine metabolism is involved in the process of OA [52]. Thus, the highly expressed genes in the chondrocytes may be closely related to the metabolisms, and deserve further investigations.

Our study has limitations. First, the difficulty in disassociating the TMJ-OA cartilage caused the small sample size, and future studies should involve more samples to confirm our conclusions. Second, the control was benign CH cartilage, which might be slightly different from normal cartilage.

In conclusion, scRNA-seq was used for the first time to identify cells and genes in a human TMJ-OA condylar cartilage. The neurovascular–osteochondral network crosstalk during the TMJ-OA process in a TMJ-OA condylar cartilage was demonstrated and discussed in-depth. Targeting the crosstalk of these processes may be a potential comprehensive therapeutic strategy for human TMJ-OA. Our findings can guide TMJ-OA etiology and treatment strategy studies.
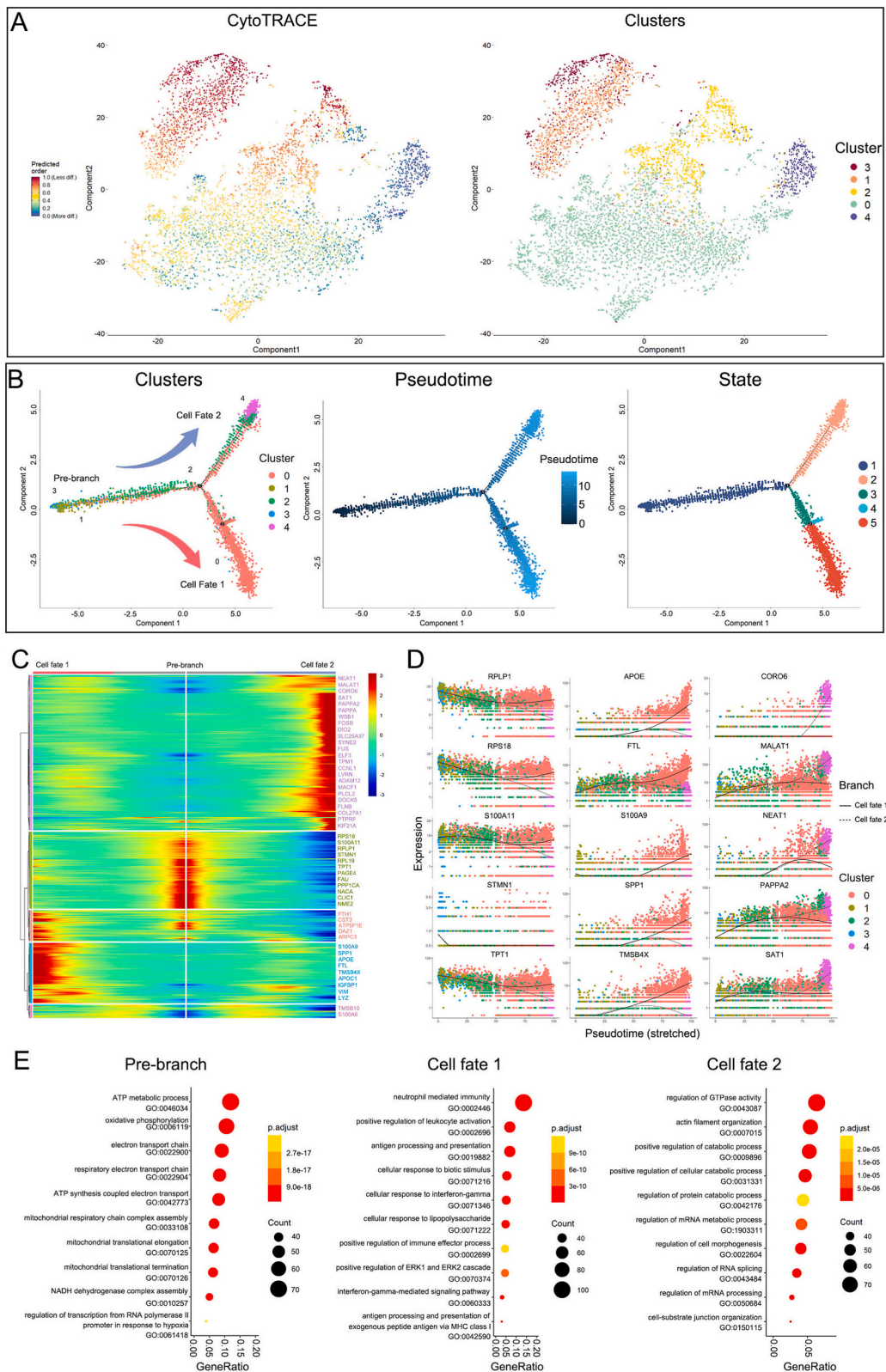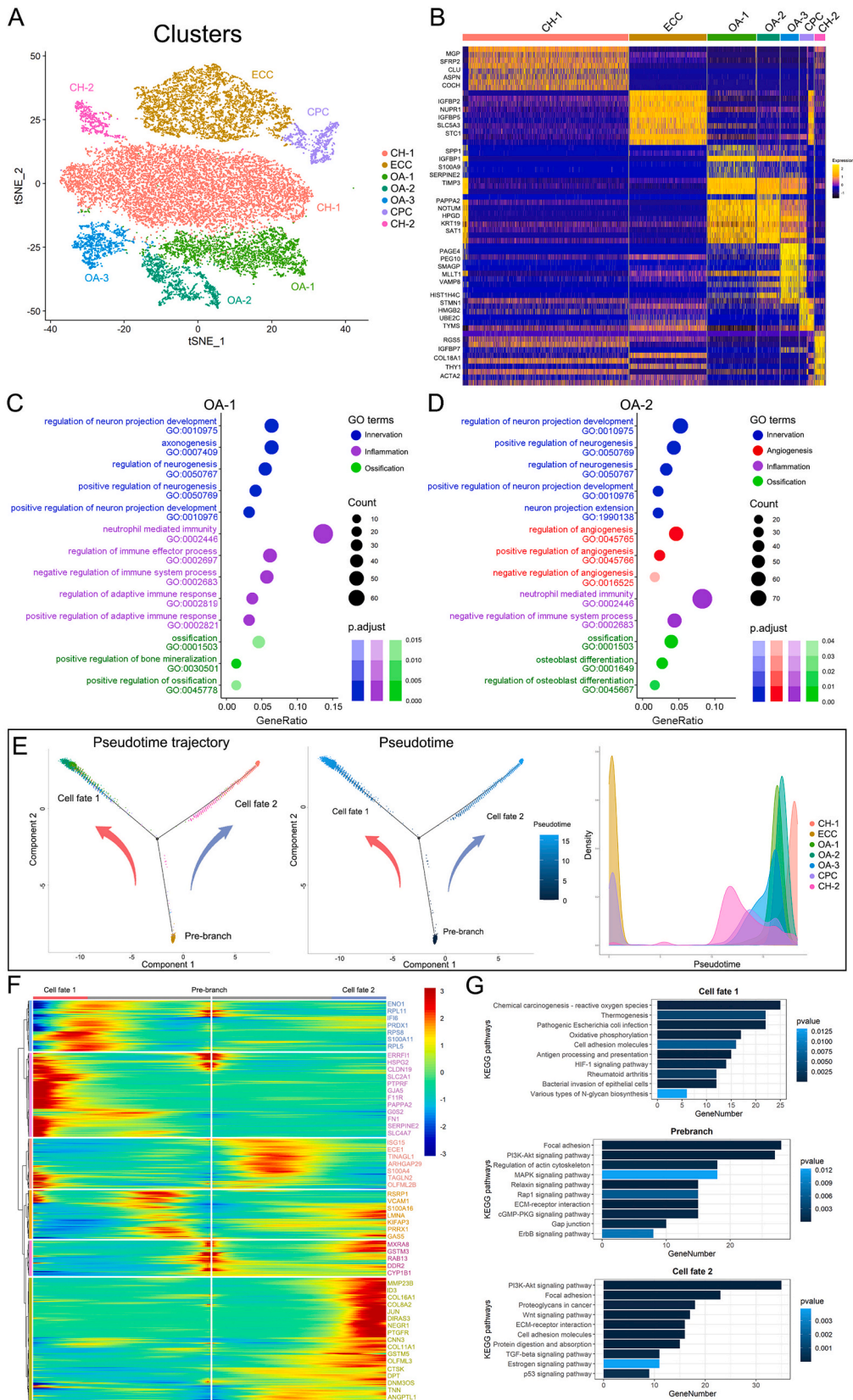
Fig. 4. Analysis of chondrocytes in OA cartilage. (A) CytoTRACE analysis of OA chondrocytes. (B) Reconstructed pseudotime trajectory of OA chondrocytes. (C, D) Highly expressed genes in Cell Fate 1, Pre-branch, and Cell Fate 2 OA chondrocytes depicted by heat map (C) and scatter plot (D), and their enriched GO terms (E).

(caption on next page)

Fig. 5. Analysis of chondrocytes in OA and CH cartilage. (A) Chondrocytes from OA and CH cartilage, and ECCs. (B) Highly expressed genes in each cluster. (C, D) GO terms related to innervation, inflammation, and ossification in cluster OA-1 (C) and OA-2 (D). (E) Reconstructed pseudotime trajectory of chondrocytes. (F) DEGs in Cell Fate 1, Pre-branch, and Cell Fate 2. (G) KEGG pathways enriched in Cell Fate 1, Pre-branch, and Cell Fate 2.
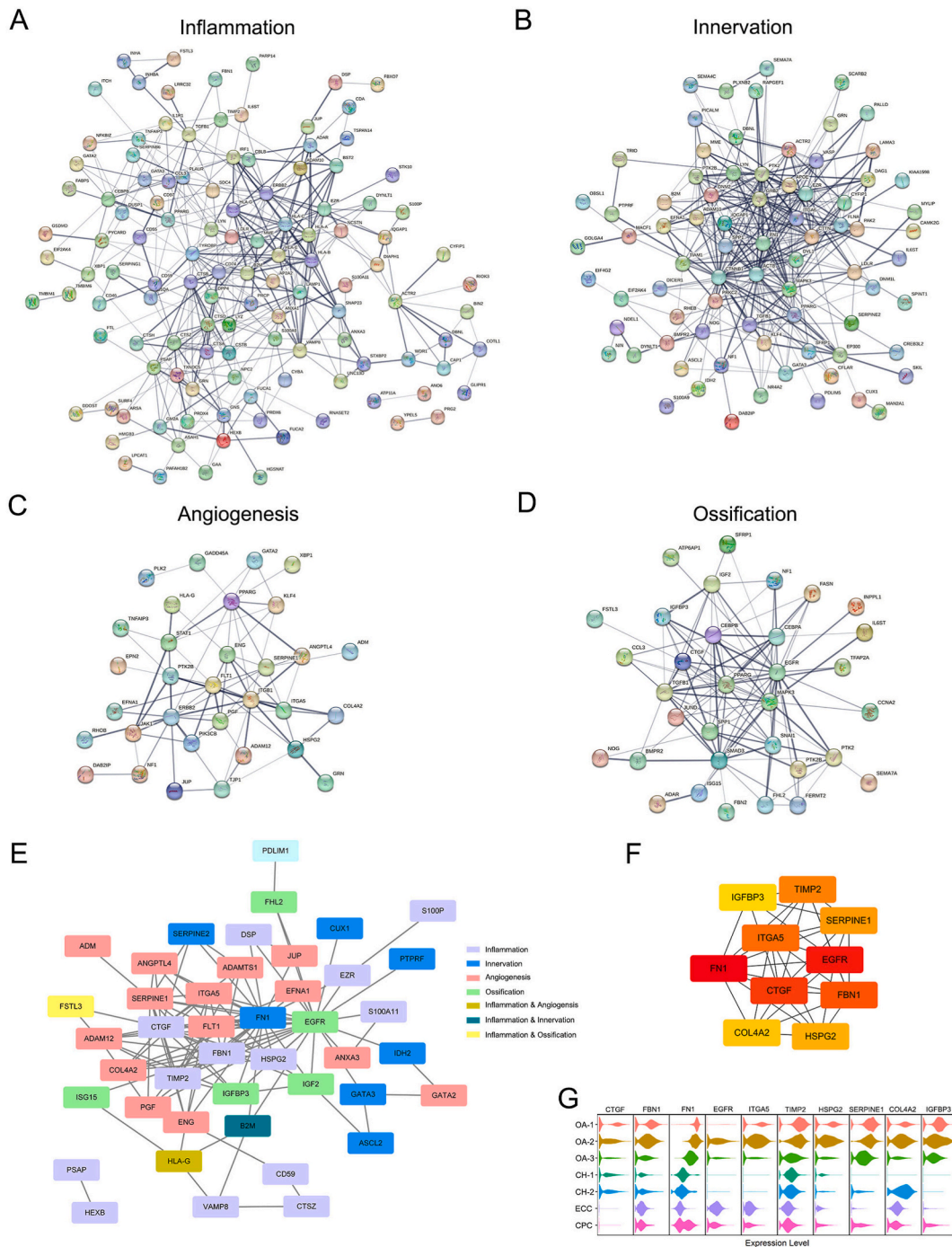

Fig. 6. PPI network analysis of DEGs in OA. (A–D) PPI network of highly expressed genes related to inflammation (A), innervation (B), angiogenesis (C), and ossification (D) in OA chondrocytes. (E) PPI network of genes with log2(fold change) > 2 among the genes. (F) PPI network of 10 hub genes. (G) Expression levels of the 10 hub genes in chondrocyte clusters.

Ethics statement

The primary human tissues were approved by the Ethics Committee of Shanghai Jiao Tong University, School of Medicine (SH9H-2019-T189-2). Signed informed consents were acquired from the patients. The study was performed in accordance with the ethical standards laid down in the 1964 Declaration of Helsinki and its later amendments.

Author contribution statement

Dahe Zhang, Yuxin Zhang: Performed the experiments; Analyzed and interpreted the data; Contributed reagents, materials, analysis tools or data; Wrote the paper. Simo Xia: Analyzed and interpreted the data. Lu Chen, Weifeng Xu, Liang Huo: Contributed reagents, materials, analysis tools or data ; Dong Huang, Pei Shen, Chi Yang: Conceived and designed the experiments; Wrote the paper.

Funding statement

Declaration of competing interest

The authors declare that they have no known competing financial interests or personal relationships that could have appeared to influence the work reported in this paper.

Appendix A. Supplementary data

Supplementary data to this article can be found online at https://doi.org/10.1016/j.heliyon.2023.e20749.

References

[1] C.L. Chang, D.H. Wang, M.C. Yang, W.E. Hsu, M.L. Hsu, Functional disorders of the temporomandibular joints: internal derangement of the temporomandibular joint, Kaohsiung J. Med. Sci. 34 (2018) 223–230, https://doi.org/10.1016/j.kjms.2018.01.004.
[2] K. Lu, F. Ma, D. Yi, H. Yu, L. Tong, D. Chen, Molecular signaling in temporomandibular joint osteoarthritis, J Orthop Translat 32 (2022) 21–27, https://doi.org/10.1016/j.jot.2021.07.001.
[3] S. Wadhwa, S. Kapila, TMJ disorders: future innovations in diagnostics and therapeutics, J. Dent. Educ. 72 (2008) 930–947.
[4] D.L. Stocum, W.E. Roberts, Part I: development and physiology of the temporomandibular joint, Curr. Osteoporos. Rep. 16 (2018) 360–368, https://doi.org/10.1007/s11914-018-0447-7.
[5] T.M. Acri, K. Shin, D. Seol, N.Z. Laird, I. Song, S.M. Geary, J.L. Chakka, J.A. Martin, A.K. Salem, Tissue engineering for the temporomandibular joint, Adv. Healthcare Mater. 8 (2019), e1801236, https://doi.org/10.1002/adhm.201801236.
[6] B. Li, G. Guan, L. Mei, K. Jiao, H. Li, Pathological mechanism of chondrocytes and the surrounding environment during osteoarthritis of temporomandibular joint, J. Cell Mol. Med. 25 (2021) 4902–4911, https://doi.org/10.1111/jcmm.16514.
[7] D. Chen, J. Shen, W. Zhao, T. Wang, L. Han, J.L. Hamilton, H.J. Im, Osteoarthritis: toward a comprehensive understanding of pathological mechanism, Bone Res 5 (2017), 16044, https://doi.org/10.1038/boneres.2016.44.
[8] Y. Zhao, L. Xie, An update on mesenchymal stem cell-centered therapies in temporomandibular joint osteoarthritis, Stem Cell. Int. 2021 (2021), 6619527, https://doi.org/10.1155/2021/6619527.
[9] W. Qin, Z. Zhang, J. Yan, X. Han, L.N. Niu, K. Jiao, Interaction of neurovascular signals in the degraded condylar cartilage, Front. Bioeng. Biotechnol. 10 (2022), 901749, https://doi.org/10.3389/fbioe.2022.901749.
[10] X.D. Wang, X.X. Kou, J.J. Mao, Y.H. Gan, Y.H. Zhou, Sustained inflammation induces degeneration of the temporomandibular joint, J. Dent. Res. 91 (2012) 499–505, https://doi.org/10.1177/0022034512441946.
[11] X.D. Wang, J.N. Zhang, Y.H. Gan, Y.H. Zhou, Current understanding of pathogenesis and treatment of TMJ osteoarthritis, J. Dent. Res. 94 (2015) 666–673, https://doi.org/10.1177/0022034515574770.
[12] Y. Hu, X. Chen, S. Wang, Y. Jing, J. Su, Subchondral bone microenvironment in osteoarthritis and pain, Bone Res 9 (2021) 20, https://doi.org/10.1038/s41413-021-00147-z.
[13] L. Chen, F. Yao, T. Wang, G. Li, P. Chen, M. Bulsara, J.J.Y. Zheng, E. Landao-Bassonga, M. Firth, P. Vasantharao, Y. Huang, M. Lorimer, S. Graves, J. Gao, R. Carey-Smith, J. Papadimitriou, C. Zhang, D. Wood, C. Jones, M. Zheng, Horizontal fissuring at the osteochondral interface: a novel and unique pathological feature in patients with obesity-related osteoarthritis, Ann. Rheum. Dis. 79 (2020) 811–818, https://doi.org/10.1136/annrheumdis-2020-216942.
[14] P.I. Mapp, D.A. Walsh, Mechanisms and targets of angiogenesis and nerve growth in osteoarthritis, Nat. Rev. Rheumatol. 8 (2012) 390–398, https://doi.org/10.1038/nrrheum.2012.80.
[15] S.A. Fenwick, P.J. Gregg, P. Rooney, Osteoarthritic cartilage loses its ability to remain avascular, Osteoarthritis Cartilage 7 (1999) 441–452, https://doi.org/10.1053/joca.1998.0238.
[16] D. Pfander, K. Gelse, Hypoxia and osteoarthritis: how chondrocytes survive hypoxic environments, Curr. Opin. Rheumatol. 19 (2007) 457–462, https://doi.org/10.1097/BOR.0b013e3282ba5693.
[17] Q.Q. Wan, W.P. Qin, Y.X. Ma, M.J. Shen, J. Li, Z.B. Zhang, J.H. Chen, F.R. Tay, L.N. Niu, K. Jiao, Crosstalk between bone and nerves within bone, Adv. Sci. 8 (2021), 2003390, https://doi.org/10.1002/advs.202003390.
[18] P. Carmeliet, M. Tessier-Lavigne, Common mechanisms of nerve and blood vessel wiring, Nature 436 (2005) 193–200, https://doi.org/10.1038/nature03875.

[19] G.D. Walker, M. Fischer, J. Gannon, R.C. Thompson, T.R. Oegema Jr., Expression of type-X collagen in osteoarthritis, J. Orthop. Res. 13 (1995) 4–12, https://doi.org/10.1002/jor.1100130104.

[20] Y. Zhao, Y. An, L. Zhou, F. Wu, G. Wu, J. Wang, L. Chen, Animal models of temporomandibular joint osteoarthritis: classification and selection, Front. Physiol. 13 (2022), 859517, https://doi.org/10.3389/fphys.2022.859517.

[21] J. Crossman, H. Lai, M. Kulka, N. Jomha, P. Flood, T. El-Bialy, Collagen-induced temporomandibular joint arthritis juvenile rat animal model, Tissue Eng. C Methods 27 (2021) 115–123, https://doi.org/10.1089/ten.TEC.2020.0294.

[22] Q. Liu, H. Yang, M. Zhang, J. Zhang, L. Lu, S. Yu, Y. Wu, M. Wang, Initiation and progression of dental-stimulated temporomandibular joints osteoarthritis, Osteoarthritis Cartilage 29 (2021) 633–642, https://doi.org/10.1016/j.joca.2020.12.016.

[23] X. Liu, H.X. Cai, P.Y. Cao, Y. Feng, H.H. Jiang, L. Liu, J. Ke, X. Long, TLR4 contributes to the damage of cartilage and subchondral bone in discectomy-induced TMJOA mice, J. Cell Mol. Med. 24 (2020) 11489–11499, https://doi.org/10.1111/jcmm.15763.

[24] Y. Zou, S. Cai, H. Lin, J. Cai, D.L. Zheng, Y.G. Lu, L. Xu, Experimental functional shift-induced osteoarthritis-like changes at the TMJ and altered integrin expression in a rat model, Ann. N. Y. Acad. Sci. 1511 (2022) 210–227, https://doi.org/10.1111/nyas.14741.

[25] P. Shen, L. Chen, D. Zhang, S. Xia, Z. Lv, D. Zou, Z. Zhang, C. Yang, W. Li, Rapid induction and long-term self-renewal of neural crest-derived ectodermal chondrogenic cells from hPSCs, NPJ Regen Med 7 (2022) 69, https://doi.org/10.1038/s41536-022-00265-0.

[26] R.C. Team, R: A Language and Environment for Statistical Computing, R Foundation for Statistical Computing, Vienna, Austria, 2021.

[27] R. Satija, J.A. Farrell, D. Gennert, A.F. Schier, A. Regev, Spatial reconstruction of single-cell gene expression data, Nat. Biotechnol. 33 (2015) 495–502, https://doi.org/10.1038/nbt.3192.

[28] C.S. McGinnis, L.M. Murrow, Z.J. Gartner, DoubletFinder: doublet detection in single-cell RNA sequencing data using artificial nearest neighbors, Cell Syst 8 (2019) 329–337.e4, https://doi.org/10.1016/j.cels.2019.03.003.

[29] I. Korsunsky, N. Millard, J. Fan, K. Slowikowski, F. Zhang, K. Wei, Y. Baglaenko, M. Brenner, P.R. Loh, S. Raychaudhuri, Fast, sensitive and accurate integration of single-cell data with Harmony, Nat. Methods 16 (2019) 1289–1296, https://doi.org/10.1038/s41592-019-0619-0.

[30] T. Wu, E. Hu, S. Xu, M. Chen, P. Guo, Z. Dai, T. Feng, L. Zhou, W. Tang, L. Zhan, X. Fu, S. Liu, X. Bo, G. Yu, clusterProfiler 4.0: a universal enrichment tool for interpreting omics data, Innovation 2 (2021), 100141, https://doi.org/10.1016/j.xinn.2021.100141.

[31] S. Hänzelmann, R. Castelo, J. Guinney, GSVA: gene set variation analysis for microarray and RNA-seq data, BMC Bioinf. 14 (2013) 7, https://doi.org/10.1186/1471-2105-14-7.

[32] X. Qiu, A. Hill, J. Packer, D. Lin, Y.A. Ma, C. Trapnell, Single-cell mRNA quantification and differential analysis with Census, Nat. Methods 14 (2017) 309–315, https://doi.org/10.1038/nmeth.4150.

[33] G.S. Gulati, S.S. Sikandar, D.J. Wesche, A. Manjunath, A. Bharadwaj, M.J. Berger, F. Ilagan, A.H. Kuo, R.W. Hsieh, S. Cai, M. Zabala, F.A. Scheeren, N.A. Lobo, D. Qian, F.B. Yu, F.M. Dirbas, M.F. Clarke, A.M. Newman, Single-cell Transcriptional Diversity Is a Hallmark of Developmental Potential, bioRxiv, 2019, 649848, https://doi.org/10.1101/649848.

[34] P. Shannon, A. Markiel, O. Ozier, N.S. Baliga, J.T. Wang, D. Ramage, N. Amin, B. Schwikowski, T. Ideker, Cytoscape: a software environment for integrated models of biomolecular interaction networks, Genome Res. 13 (2003) 2498–2504, https://doi.org/10.1101/gr.1239303.

[35] Z.F. Xiao, G.Y. Su, Y. Hou, S.D. Chen, D.K. Lin, Cartilage degradation in osteoarthritis: a process of osteochondral remodeling resembles the endochondral ossification in growth plate? Med. Hypotheses 121 (2018) 183–187, https://doi.org/10.1016/j.mehy.2018.08.023.

[36] Y. Peng, S. Wu, Y. Li, J.L. Crane, Type H blood vessels in bone modeling and remodeling, Theranostics 10 (2020) 426–436, https://doi.org/10.7150/thno.34126.

[37] Z. Yang, W. Li, C. Song, H. Leng, CTGF as a multifunctional molecule for cartilage and a potential drug for osteoarthritis, Front. Endocrinol. 13 (2022), 1040526, https://doi.org/10.3389/fendo.2022.1040526.

[38] M. van Hoolwerff, M. Tuerlings, I.J.L. Wijnen, H.E.D. Suchiman, D. Cats, H. Mei, R. Nelissen, H.M.J. van der Linden-van der Zwaag, Y.F.M. Ramos, R. Coutinho de Almeida, I. Meulenbelt, Identification and functional characterization of imbalanced osteoarthritis associated fibronectin splice variants, Rheumatology (2022), https://doi.org/10.1093/rheumatology/keac272.

[39] Y. Wei, L. Luo, T. Gui, F. Yu, L. Yan, L. Yao, L. Zhong, W. Yu, B. Han, J.M. Patel, J.F. Liu, F. Beier, L.S. Levin, C. Nelson, Z. Shao, L. Han, R.L. Mauck, A. Tsourkas, J. Ahn, Z. Cheng, L. Qin, Targeting cartilage EGFR pathway for osteoarthritis treatment, Sci. Transl. Med. 13 (2021), https://doi.org/10.1126/scitranslmed.abb3946.

[40] H. Kaneko, M. Ishijima, I. Futami, N. Tomikawa-Ichikawa, K. Kosaki, R. Sadatsuki, Y. Yamada, H. Kurosawa, K. Kaneko, E. Arikawa-Hirasawa, Synovial perlecan is required for osteophyte formation in knee osteoarthritis, Matrix Biol. 32 (2013) 178–187, https://doi.org/10.1016/j.matbio.2013.01.004.

[41] Y. Wen, H. Yang, J. Wu, A. Wang, X. Chen, S. Hu, Y. Zhang, D. Bai, Z. Jin, COL4A2 in the tissue-specific extracellular matrix plays important role on osteogenic differentiation of periodontal ligament stem cells, Theranostics 9 (2019) 4265–4286, https://doi.org/10.7150/thno.35914.

[42] S. Yu, L. Sun, L. Liu, K. Jiao, M. Wang, Differential expression of IGF1, IGFR1 and IGFBP3 in mandibular condylar cartilage between male and female rats applied with malocclusion, J. Oral Rehabil. 39 (2012) 727–736, https://doi.org/10.1111/j.1365-2842.2012.02332.x.

[43] K. Sun, J. Luo, J. Guo, X. Yao, X. Jing, F. Guo, The PI3K/AKT/mTOR signaling pathway in osteoarthritis: a narrative review, Osteoarthritis Cartilage 28 (2020) 400–409, https://doi.org/10.1016/j.joca.2020.02.027.

[44] R. Mathew, C.M. Karp, B. Beaudoin, N. Vuong, G. Chen, H.Y. Chen, K. Bray, A. Reddy, G. Bhanot, C. Gelinas, R.S. Dipaola, V. Karantza-Wadsworth, E. White, Autophagy suppresses tumorigenesis through elimination of p62, Cell 137 (2009) 1062–1075, https://doi.org/10.1016/j.cell.2009.03.048.

[45] Ł. Łapaj, J. Markuszewski, M. Wierusz-Kozłowska, [Current views on the pathogenesis of osteoarthritis], Chir. Narzadow Ruchu Ortop. Pol. 75 (2010) 248–260.

[46] J. Lu, H. Zhang, D. Cai, C. Zeng, P. Lai, Y. Shao, H. Fang, D. Li, J. Ouyang, C. Zhao, D. Xie, B. Huang, J. Yang, Y. Jiang, X. Bai, Positive-feedback regulation of subchondral H-type vessel formation by chondrocyte promotes osteoarthritis development in mice, J. Bone Miner. Res. 33 (2018) 909–920, https://doi.org/10.1002/jbmr.3388.

[47] F. Sasazawa, T. Onodera, T. Yamashita, N. Seito, Y. Tsukuda, N. Fujitani, Y. Shinohara, N. Iwasaki, Depletion of gangliosides enhances cartilage degradation in mice, Osteoarthritis Cartilage 22 (2014) 313–322, https://doi.org/10.1016/j.joca.2013.11.015.

[48] G. Zhai, R. Wang-Sattler, D.J. Hart, N.K. Arden, A.J. Hakim, T. Illig, T.D. Spector, Serum branched-chain amino acid to histidine ratio: a novel metabolomic biomarker of knee osteoarthritis, Ann. Rheum. Dis. 69 (2010) 1227–1231, https://doi.org/10.1136/ard.2009.120857.

[49] N.G. Sitton, J.S. Dixon, H.A. Bird, V. Wright, Serum and synovial fluid histidine: a comparison in rheumatoid arthritis and osteoarthritis, Rheumatol. Int. 6 (1986) 251–254, https://doi.org/10.1007/bf00541315.

[50] Z. Huang, Z. He, Y. Kong, Z. Liu, L. Gong, Insight into osteoarthritis through integrative analysis of metabolomics and transcriptomics, Clin. Chim. Acta 510 (2020) 323–329, https://doi.org/10.1016/j.cca.2020.07.010.

[51] M. Binvignat, P. Emond, F. Mifsud, B. Miao, A. Courties, A. Lefèvre, E. Maheu, M.D. Crema, D. Klatzmann, M. Kloppenburg, P. Richette, A.J. Butte, E. Mariotti-Ferrandiz, F. Berenbaum, H. Sokol, J. Sellam, Serum tryptophan metabolites are associated with erosive hand osteoarthritis and pain: results from the DIGICOD cohort, Osteoarthritis Cartilage 31 (2023) 1132–1143, https://doi.org/10.1016/j.joca.2023.04.007.

[52] M.N. Ferrao Blanco, H. Domenech Garcia, L. Legeai-Mallet, G. van Osch, Tyrosine kinases regulate chondrocyte hypertrophy: promising drug targets for Osteoarthritis, Osteoarthritis Cartilage 29 (2021) 1389–1398, https://doi.org/10.1016/j.joca.2021.07.003.